# Global in time stability and accuracy of IMEX-FEM data assimilation schemes for Navier-Stokes equations

Adam Larios * Leo G. Rebholz† Camille Zerfas ‡

**Abstract**

We study numerical schemes for incompressible Navier-Stokes equations using IMEX temporal discretizations, finite element spatial discretization, and equipped with continuous data assimilation (a technique recently developed by Azouani, Olson, and Titi in 2014). We analyze stability and accuracy of the proposed methods, and are able to prove well-posedness, long time stability, and long time accuracy estimates, under restrictions of the time step size and data assimilation parameter. We give results for several numerical tests that illustrate the theory, and show that for good results the choice of discretization parameter and element choices can be critical.

## 1 Introduction

Data assimilation (DA) refers to a wide class of schemes for incorporating observational data in simulations in order to increase the accuracy of solutions and to obtain better estimates of initial conditions. It is the subject of a large body of work (see, e.g., [11, 30, 34], and the references therein). DA algorithms are widely used in weather modeling, climate science, and hydrological and environmental forecasting [29]. Classically, these techniques are based on linear quadratic estimation, also known as the Kalman Filter. The Kalman Filter is described in detail in several textbooks, including [11, 30, 34, 9], and the references therein. Recently, a promising new approach to data assimilation was pioneered by Azouani, Olson, and Titi [3, 4] (see also [8, 24, 41] for early ideas in this direction). This new approach, which we call AOT Data Assimilation or continuous data assimilation, adds a feedback control term at the PDE level that nudges the computed solution towards the reference solution corresponding to the observed data. A similar approach is taken by Blömker, Law, Stuart, and Zygalakis in [7] in the context of stochastic differential equations. The AOT algorithm is based on feedback control at the PDE (partial differential equation) level, described below. The first works in this area assumed noise-free observations, but [5] adapted the method to the case of noisy data, and [17] adapted to the case in which measurements are obtained discretely in time and may be contaminated by systematic errors. Computational experiments on this technique were carried out in the cases of the 2D Navier-Stokes equations [19], the 2D Bénard

*Department of Mathematics, University of Nebraska-Lincoln, Lincoln, NE 68588; email: alarios@unl.edu, partially supported by NSF Grant DMS 1716801

†Department of Mathematical Sciences, Clemson University, Clemson, SC, 29634; email: rebholz@clemson.edu, partially supported by NSF Grant DMS 1522191.

‡Department of Mathematical Sciences, Clemson University, Clemson, SC, 29634; email: czerfas@clemson.edu, partially supported by NSF Grant DMS 1522191.

convection equations [2], the 1D Kuramoto-Sivashinsky equations [36], and the 3D Navier-Stokes equations [32].

Computational experiments on the AOT algorithm and its variants were carried out in the cases of the 2D Navier-Stokes equations [19], the 2D Bénard convection equations [2], and the 1D Kuramoto-Sivashinsky equations [36, 31]. In [31], several nonlinear versions of this approach were proposed and studied. In addition to the results discussed here, a large amount of recent literature has built upon this idea; see, e.g., [1, 6, 12, 13, 14, 15, 16, 18, 21, 27, 28, 33, 37, 39].

Although extensive research has been done on the theory of DA algorithms, there is currently little work on the numerical analysis of these algorithms, save [40], which studied a continuous-in-time Galerkin approximation of the algorithm. In this paper, we will be analyzing discrete numerical algorithms of the Navier-Stokes equations (NSE) with an added data assimilation term and grad-div term. Briefly, the 2D incompressible NSE are given by

$$u_t + (u\cdot\nabla)u - \nu\Delta u + \nabla p + \gamma\nabla(\nabla\cdot u) = f, \tag{1.1} \quad \boxed{\texttt{nse1}}$$

$$\nabla\cdot u = 0, \tag{1.2} \quad \boxed{\texttt{nse2}}$$

where $u$ represents the velocity and $p$ pressure. The viscosity is given by $\nu > 0$, and external forcing is $f$. Note that at the continuous level, the grad-div term is zero. The corresponding data assimilation algorithm is given by the system,

$$v_t + (v\cdot\nabla)v + \nabla q - \nu\Delta v + \mu I_H(v-u) + \gamma\nabla(\nabla\cdot v) = f, \tag{1.3} \quad \boxed{\texttt{contDA1}}$$

$$\nabla\cdot v = 0, \tag{1.4} \quad \boxed{\texttt{contDA2}}$$

where $v$ is the approximate velocity and $q$ the pressure of this approximate flow. The viscosity $\nu > 0$ and forcing $f$ are the same as the above. The scalar $\mu$ is known as the nudging parameter, and $I_h$ is the interpolation operator, where $h$ is the resolution of the coarse spatial mesh. The added data assimilation term forces (or nudges) the coarse spacial scales of the approximating solution $v$ to the coarse spatial scales of the true solution $u$. The initial value of $v$ is arbitrary.

We note that in all computational studies discussed above, the equations have been handled with fully explicit schemes (typically forward Euler). However, in explicit schemes, numerical instability is expected to arise from the term $\mu I_H(v-u)$ on the right-hand side of (1.4) for large values of $\mu$, and thus an implicit treatment of this term has advantages. Thus, we study a backward Euler scheme for the data assimilation algorithm below. Fully implicit schemes can be costly though, due to the need to solve nonlinear systems, which can require, e.g., expensive Newton solves at every time step. Therefore, we also study implicit-explicit (IMEX) schemes, which handle the nonlinear term semi-implicitly, but the linear terms (in particular, $\mu I_H(v-u)$) implicitly.

This paper is organized as follows. In section 2, we will introduce the necessary notation and preliminary results needed in the proceeding sections. Section 3 introduces a linear first order scheme of the 2D NSE with a grad-div term. We then show stability of the algorithms and optimal convergence rates of the data assimilation algorithm to the true NSE solution. Similarly, section 4 includes the convergence analysis of a linear second order numerical scheme of the 2D NSE with a data assimilation term. Lastly, section 5 contains three numerical tests that illustrate the optimal convergence rates, and issues that arise in numerical implementation that one may not see from the analysis of the scheme.

## 2 Notation and Preliminaries

We consider a bounded domain $\Omega \subset \mathbb{R}^d$ with $d$=2 or 3. The $L^2(\Omega)$ norm and inner product will be denoted by $\|\cdot\|$ and $(\cdot,\cdot)$, respectively, while all other norms will be labeled with subscripts.

Denote the natural function spaces for velocity and pressure, respectively, by

$$\begin{aligned} X &:= H_0^1(\Omega)^d \\ Q &:= L_0^2(\Omega). \end{aligned}$$

In $X$, we have the Poincaré inequality: there exists a constant $C_P$ depending only on $\Omega$ such that for any $\phi \in X$,

$$\|\phi\| \leq C_P \|\nabla \phi\|.$$

The dual norm of $X$ will be denoted by $\|\cdot\|_{-1}$.

We denote the trilinear form $b : X \times X \times X \to \mathbb{R}$, which is defined on smooth functions $u, v, w$ by

$$b(u,v,w) = \frac{1}{2}(u \cdot \nabla v, w) - \frac{1}{2}(u \cdot \nabla w, v).$$

An equivalent form of $b$ on $X \times X \times X$ can be constructed as

$$b(u,v,w) = (u \cdot \nabla v, w) + \frac{1}{2}((\nabla \cdot u)v, w).$$

An important property of the $b$ operator is that $b(u,v,v) = 0$ for $u, v \in X$.

We will utilize the following bounds on $b$.

bbounds **Lemma 2.1.** *There exists a constant $M$ dependent only on $\Omega$ satisfying*

$$\begin{aligned} |b(u,v,w)| &\leq M \|\nabla u\| \|\nabla v\| \|\nabla w\|, \\ |b(u,v,w)| &\leq M \|u\| (\|\nabla v\|_{L^3} + \|v\|_{L^\infty}) \|\nabla w\|, \end{aligned}$$

*for all $u, v, w \in X$ for which the norms on the right hand sides are finite.*

*Proof.* These well known bounds follow from Hölder's inequality, Sobolev inequalities, and the Poincaré inequality. ☐

### 2.1 Discretization preliminaries

Denote by $\tau_h$ a regular, conforming triangulation of the domain $\Omega$, and let $X_h \subset X$, $Q_h \subset Q$ be an inf-sup stable pair of discrete velocity - pressure spaces. For simplicity, we will take $X_h = X \cap P_k$ and $Q_h = Q \cap P_{k-1}$ Taylor-Hood or Scott-Vogelius elements however our results in the following sections are extendable to most other inf-sup stable element choices.

We assume the mesh is sufficiently regular for the inverse inequality to hold: there exists a constant $C$ such that for all $v_h \in X_h$,

$$\|\nabla v_h\| \leq C h^{-1} \|v_h\|.$$

Define the discretely divergence free subspace by

$$V_h := \{v_h \in X_h \mid (\nabla \cdot v_h, q_h) = 0 \ \forall \ q_h \in Q_h\}.$$

We denote $I_H$ be an interpolation operator satisfying

$$\|I_H(\phi) - \phi\| \leq C_I h \|\nabla \phi\| \tag{2.2}$$

interp1

$$\|I_H(\phi)\| \leq C\|\phi\| \tag{2.3}$$

interp2

for all $\phi \in X$. Here, $H$ is a characteristic point spacing for the interpolant, and will satisfy $h \leq H$, $H = ch$. The spacing $H$ corresponds in practice to points where (true solution) measurements are taken, so $H$ should be as large as possible but still satisfying (2.2)-(2.3).

Throughout this paper, the nudging parameter $\mu > 0$ is assumed to satisfy the upper bound

$$\mu \;\leq\; \frac{\nu}{2} C_I^{-2} h^{-2}. \tag{2.4}$$

However, we remark that $\mu$ *does not scale with* $h$ *as* $h \to 0$. The mesh width $h$ may need to be sufficient small for the algorithms to work (as $\mu$ will also be bounded below by a data dependent constant in the theorems to follow), but once $h$ is 'small enough', $\mu$ need not increase if $h$ decreases further.

We also define the quantity

$$\alpha := \nu - 2\mu C_I^2 h^2,$$

and will equivalently assume that $\alpha > 0$. Note that $\mu$ will also have a data dependent lower bound, but choosing $h$ small enough will guarantee the existence of an appropriate $\mu$.

## 2.2 Additional preliminaries

Several results in this paper utilize the following inequality for sequences.

geoseries

**Lemma 2.5.** *Suppose constants* $r$ *and* $B$ *satisfy* $r > 1$, $B \geq 0$. *Then if the sequence of real numbers* $\{a_n\}$ *satisfies*

$$r a_{n+1} \leq a_n + B, \tag{2.6}$$

sequence

*we have that*

$$a_{n+1} \leq a_0 \left(\frac{1}{r}\right)^{n+1} + \frac{B}{r-1}.$$

*Proof.* The inequality (2.6) can be written as

$$a_{n+1} \leq \frac{a_n}{r} + \frac{B}{r}.$$

Recursively, we obtain

$$\begin{aligned}
a_{n+1} &\leq \frac{1}{r}\left(\frac{a_{n-1}}{r} + \frac{B}{r}\right) + \frac{B}{r} \\
&= \frac{a_{n-1}}{r^2} + \frac{B}{r}\left(1 + \frac{1}{r}\right) \\
&\vdots \\
&\leq \frac{a_0}{r^{n+1}} + \frac{B}{r}\left(1 + \frac{1}{r} + \cdots + \frac{1}{r^n}\right).
\end{aligned}$$

Now the resulting finite geometric series is bounded as

$$\frac{B}{r}\left(1+\frac{1}{r}+\cdots+\frac{1}{r^n}\right)=\frac{B}{r}\cdot\frac{1-(1/r)^{n+1}}{1-(1/r)}\leq\frac{B}{r}\cdot\frac{1}{1-(1/r)}\leq\frac{B}{r-1},$$

which gives the result. $\square$

The analysis in section 4 that uses a BDF2 approximation to the time derivative term will use the $G$-norm, which is commonly used in BDF2 analysis, see e.g. [22], [10]. Define the matrix

$$G=\begin{bmatrix}1/2 & -1\\ -1 & 5/2\end{bmatrix},$$

and note that $G$ induces the norm $\|x\|_G^2 := (x, Gx)$, which is equivalent to the $(L^2)^2$ norm:

$$C_l\|x\|_G \leq \|x\| \leq C_u\|x\|_G.$$

The following property is well-known [22]. Set $\chi_v^n := [v^{n-1}, v^n]^T$, if $v^i \in L^2(\Omega)$, $i = n-1, n$, we have

$$\left(\frac{1}{2}(3v^{n+1}-4v^n+v^{n-1}), v^{n+1}\right)=\frac{1}{2}(\|\chi_v^{n+1}\|_G^2-\|\chi_v^n\|_G^2)+\frac{1}{4}\|v^{n+1}-2v^n+v^{n-1}\|^2. \tag{2.7}$$ Gidentity

# 3 A first order IMEX-FEM scheme and its analysis

We consider now an efficient fully discretized scheme for (1.3)-(1.4). We use a first order temporal discretization for the purposes of simplicity of analysis, and in the next section we consider the extension to second order time stepping. The time stepping method employed is backward Euler, but linearized at each time step by lagging part of the convective term in time. The spatial discretization is the finite element method, and we assume the velocity-pressure finite element spaces $(X_h, Q_h) = (P_k, P_{k-1})$ for simplicity (although extension to any LBB-stable pair can be done without significant difficulty). We also utilize grad-div stabilization, with parameter $\gamma$, and will assume $\gamma = O(1)$. For most common element choices, grad-div stabilization is well-known to improve mass conservation and reduce the effect of the pressure on the velocity error [26]; a similar effect is observed in the convergence result for this DA scheme, as well as in the numerical tests. In this section, we prove well-posedness of the scheme, as well as an error estimate, both of which are uniform in $n$ (global in time), provided some restrictions on the nudging parameter and on the time step size.

We now define the first order IMEX discrete DA algorithm for NSE.

alg1a **Algorithm 3.1.** Given $v_h^0 \in V_h$, $f \in L^\infty(0,\infty; L^2(\Omega))$ and $u \in L^\infty(0,\infty, L^2(\Omega))$, find $(v_h^{n+1}, q_h^{n+1}) \in (X_h, Q_h)$ for $n = 0, 1, 2, ...$, satisfying

$$\begin{aligned}\frac{1}{\Delta t}\left(v_h^{n+1}-v_h^n,\chi_h\right)+b(v_h^n,v_h^{n+1},\chi_h)-(q_h^{n+1},\nabla\cdot\chi_h)+\gamma(\nabla\cdot v_h^{n+1},\nabla\cdot\chi_h)&\\ +\nu(\nabla v_h^{n+1},\nabla\chi_h)+\mu(I_H(v_h^{n+1}-u^{n+1}),\chi_h)&=(f^{n+1},\chi_h) \quad (3.1)\\ (\nabla\cdot v_h^{n+1},r_h)&=0, \quad (3.2)\end{aligned}$$

for all $(\chi_h, r_h) \in X_h \times Q_h$.

We first prove that Algorithm 3.1 is well-posed, globally in time, without any restriction on the time step size $\Delta t$.

tabilityBE **Lemma 3.3.** *Suppose $\mu$ satisfies*

$$1 \leq \mu < \frac{\nu}{2C_I^2 h^2}.$$

*Then for any time step size $\Delta t > 0$, Algorithm 3.1 is well-posed globally in time, and solutions are nonlinearly long-time stable: for any $n > 0$,*

$$\|v_h^n\|^2 \leq \left( \frac{1}{1 + (\lambda + \mu)\Delta t} \right)^n \|v_h^0\|^2 + C(\nu^{-1} F + U) \leq C(data),$$

*where $\lambda = C_P^{-2}\alpha > 0$, $F := \|f\|^2_{L^\infty(0,\infty;H^{-1})}$, and $U := \|u\|^2_{L^\infty(0,\infty;L^2)}$.*

**Remark 3.4.** Such a choice of $\mu$ may not be possible for any $h$, but will exist for $h$ sufficiently small.

*Proof.* Since the scheme is linear and finite dimensional, proving the stability bound in Lemma 3.3 will imply global in time well-posedness.

We begin the proof for the stability bound by choosing $\chi_h = v_h^{n+1}$ in Algorithm 3.1, which vanishes the pressure and nonlinear terms. We then add and subtract $v_h^{n+1}$ in the first component of the nudging term, which yields (after dropping the non-negative terms $\gamma\|\nabla \cdot v_h^{n+1}\|^2$ and $\frac{1}{2\Delta t} + \|v_h^{n+1} - v_h^n\|^2$ on the left)

$$\begin{aligned} \frac{1}{2\Delta t}[\|v_h^{n+1}\|^2 - \|v_h^n\|^2] + \nu\|\nabla v_h^{n+1}\|^2 + \mu\|v_h^{n+1}\|^2 \\ \leq (f^{n+1}, v_h^{n+1}) - \mu(I_H v_h^{n+1} - v_h^{n+1}, v_h^{n+1}) + \mu(I_H u^{n+1}, v_h^{n+1}). \end{aligned} \tag{3.5}$$

stab1

The first term on the right hand side is bounded using the dual norm of $X$ and Young's inequality, which yields

$$(f^{n+1}, v_h^{n+1}) \leq \|f^{n+1}\|_{-1}\|\nabla v_h^{n+1}\| \leq \frac{\nu^{-1}}{2}\|f^{n+1}\|_{-1}^2 + \frac{\nu}{2}\|\nabla v_h^{n+1}\|.$$

The second term is bounded using Cauchy-Schwarz, interpolation property (2.2), and Young's inequality, after which we have that

$$\begin{aligned} \mu(I_H v_h^{n+1} - v_h^{n+1}, v_h^{n+1}) &\leq \mu\|I_H v_h^{n+1} - v_h^{n+1}\|\|v_h^{n+1}\| \\ &\leq \mu C_I^2 h^2\|\nabla v_h^{n+1}\|^2 + \frac{\mu}{4}\|v_h^{n+1}\|^2. \end{aligned}$$

Finally, the last right hand side term will be bounded with these same inequalities, and property (2.3), to obtain

$$\begin{aligned} \mu(I_H u^{n+1}, v_h^{n+1}) &\leq \mu\|I_H u^{n+1}\|\|v_h^{n+1}\| \\ &\leq C\mu\|u^{n+1}\|^2 + \frac{\mu}{4}\|v_h^{n+1}\|^2. \end{aligned}$$

Combine the above bounds for the right hand side of (3.5), then multiply both sides by $2\Delta t$ and reduce, to get

$$\begin{aligned} \|v_h^{n+1}\|^2 - \|v_h^n\|^2 + 2\alpha\Delta t\alpha\|\nabla v_h^{n+1}\|^2 + \mu\Delta t\|v_h^{n+1}\|^2 \\ \leq C\nu^{-1}\Delta t\|f^{n+1}\|_{-1}^2 + C\mu\Delta t\|u^{n+1}\|^2, \end{aligned} \tag{3.6}$$

stab2

recalling that $\alpha = \nu - 2\mu C_I^2 h^2 > 0$. Applying the Poincaré inequality to the viscous term, denoting $\lambda = 2C_P^{-2}\alpha$, and using the assumed regularity of $f$ and $u$ provides the bound

$$(1 + (\lambda + \mu)\Delta t)\|v_h^{n+1}\|^2 \le \|v_h^n\|^2 + \Delta t C(\nu^{-1}F + \mu U).$$

Next apply Lemma 2.5 to find that

$$\begin{aligned}\|v_h^{n+1}\|^2 &\le \left(\frac{1}{1+(\lambda+\mu)\Delta t}\right)^{n+1}\|v_h^0\|^2 + \frac{\Delta t C(\nu^{-1}F + \mu U)}{\Delta t(\lambda+\mu)} \\ &\le \left(\frac{1}{1+(\lambda+\mu)\Delta t}\right)^{n+1}\|v_h^0\|^2 + C(\lambda+\mu)^{-1}\nu^{-1}F + CU.\end{aligned}$$

Finally, since we assume $\mu \ge 1$, we obtain a bound for $v_h^{n+1}$, uniform in $n$:

$$\|v_h^{n+1}\|^2 \le \left(\frac{1}{1+(\lambda+\mu)\Delta t}\right)^{n+1}\|v_h^0\|^2 + C(\nu^{-1}F + U) \le C(data).$$

This stability bound is sufficient to guarantee solutions at each time step are unique. Since the scheme is linear and finite dimensional at each time step, this also implies existence and uniqueness. Finally, since the stability bound is uniform in $n$, we have global in time well-posedness of the scheme. □

We will now prove that solutions to Algorithm 3.1 converge to the true NSE solution at a rate of $\Delta t + h^k$, globally in time, provided restrictions on $\Delta t$ and $\mu$ are satisfied.

conv2 **Theorem 3.7.** *Let $u, p$ solve the NSE (1.1)-(1.2) with given $f \in L^\infty(0,\infty; L^2(\Omega))$ and $u_0 \in L^2(\Omega)$, with $u \in L^\infty(0,\infty; H^{k+1}(\Omega))$, $p \in L^\infty(0,\infty; H^k(\Omega))$ $(k \ge 1)$, $u_t \in L^\infty(0,\infty; L^2(\Omega))$, and $u_{tt} \in L^\infty(0,\infty; H^1(\Omega))$. Denote $U := |u|_{L^\infty(0,\infty;H^{k+1})}$ and $P := |p|_{L^\infty(0,\infty;H^k)}$. Assume the time step size satisfies*

$$\Delta t < CM^2\nu^{-1}\left(h^{2k-2}U^2 + \|\nabla u^{n+1}\|_{L^3}^2 + \|u^{n+1}\|_{L^\infty}^2\right)^{-1},$$

*and the parameter $\mu$ satisfies*

$$CM^2\nu^{-1}\left(h^{2k-2}U^2 + \|\nabla u^{n+1}\|_{L^3}^2 + \|u^{n+1}\|_{L^\infty}^2\right) < \mu < \frac{2\nu}{C_I^2 h^2}.$$

*Then the error in solutions to Algorithm 3.1 satisfies, for any $n$,*

$$\|u^n - v_h^n\|^2 \le \left(\frac{1}{1+2\lambda\Delta t}\right)^n \|u_0 - v_h^0\|^2 + \frac{R}{2\lambda},$$

*where $\lambda = \alpha C_P^{-2}$ and*

$$R = C\left((1+M^2)\nu^{-1}\Delta t^2 + h^{2k}U^2(M^2\nu^{-1} + M^2\nu^{-1}h^{2k}U^2 + \nu + \gamma + \nu C_I^{-2})\right).$$

**Remark 3.8.** For the case of Taylor-Hood elements and 0 initial condition in the DA algorithm, the result of the theorem reduces to

$$\|u^n - v_h^n\| \le C\left(\left(\frac{1}{1+2\lambda\Delta t}\right)^{n/2}\|u_0\| + \Delta t + h^k\right).$$

**Remark 3.9.** The time step restriction is a consequence of the IMEX time stepping. If we instead consider the fully nonlinear scheme, i.e. with $b(v_h^n, v_h^{n+1}, \chi_h)$ replaced by $b(v_h^{n+1}, v_h^{n+1}, \chi_h)$, then no $\Delta t$ restriction is required for a similar result to hold. However, in this case, the well-posedness results above would require different proof techniques, and seemingly a time step restriction would be necessary for solution uniqueness.

**Remark 3.10.** Similar to the case of NSE-FEM without DA, grad-div stabilization reduces the effect of the pressure on the $L^2$ DA solution error. With grad-div, the contribution of the error term is $h^k\gamma^{-1/2}|p|_{L^\infty(0,\infty;H^k)}$, but without it, the $\gamma^{-1/2}$ would be replaced by a $\nu^{-1/2}$. If divergence-free elements were used, then this term would completely vanish.

*Proof.* Throughout this proof, the constant $C$ will denote a generic constant, possibly changing at each instance, that is independent of $h$, $\mu$, and $\Delta t$.

Using Taylor's theorem, the NSE (true) solution satisfies, for all $\chi_h \in X_h$,

$$\begin{aligned}\frac{1}{\Delta t}\left(u^{n+1}-u^n, \chi_h\right) &+ b(u^n, u^{n+1}, \chi_h) - (p^{n+1}, \nabla\cdot\chi_h) + \gamma(\nabla\cdot u^{n+1}, \nabla\cdot\chi_h)\\ &+ \nu(\nabla u^{n+1}, \nabla\chi_h) = (f^{n+1}, \chi_h) + \frac{\Delta t}{2}(u_{tt}(t^*), \chi_h) + \Delta t b(u_t(t^{**}), u^{n+1}, \chi_h), \end{aligned} \tag{3.11}$$

nsetrue3

where $t^*, t^{**} \in [t^n, t^{n+1}]$. Subtracting (3.1) from (3.11) yields the following difference equation, with $e^n := u^n - v_h^n$:

$$\begin{aligned}\frac{1}{\Delta t}\left(e^{n+1}-e^n, \chi_h\right) &+ b(e^n, u^{n+1}, \chi_h) + b(v_h^n, e^{n+1}, \chi_h) - (p^{n+1} - q_h^n, \nabla\cdot\chi_h) + \gamma(\nabla\cdot e^{n+1}, \nabla\cdot\chi_h)\\ &+ \nu(\nabla e^{n+1}, \nabla\chi_h) + \mu(I_H(e^{n+1}), \chi_h) = \frac{\Delta t}{2}(u_{tt}(t^*), \chi_h) + \Delta t b(u_t(t^{**}), u^{n+1}, \chi_h). \end{aligned} \tag{3.12}$$

daerr1

Denote $P_{V_h}^{L^2}(u^n)$ as the $L^2$ projection of $u^n$ into the discretely divergence-free space $V_h$. We decompose the error as $e^n = u^n - P_{V_h}^{L^2}(u^n) + P_{V_h}^{L^2}(u^n) - v_h^n =: \eta^n + \phi_h^n$, and then choose $\chi_h = \phi_h^{n+1}$, which yields

$$\begin{aligned}\frac{1}{2\Delta t}[\|\phi_h^{n+1}\|^2 - \|\phi_h^n\|^2 + \|\phi_h^{n+1}-\phi_h^n\|^2] &+ \nu\|\nabla\phi_h^{n+1}\|^2 + \mu(I_H(\phi_h^{n+1}), \phi_h^{n+1}) + \gamma\|\nabla\cdot\phi_h^{n+1}\|^2\\ &= -\frac{\Delta t}{2}(u_{tt}(t^*), \phi_h^{n+1}) - \Delta t b(u_t(t^{**}), \nabla u^{n+1}, \phi_h^{n+1}) - b(v_h^n, \eta^{n+1}, \phi_h^{n+1})\\ &\quad - b(\eta^n, u^{n+1}, \phi_h^{n+1}) - b(\phi_h^n, u^{n+1}, \phi_h^{n+1}) - \mu(I_H(\eta^{n+1}), \phi_h^{n+1})\\ &\quad - (p^{n+1} - r_h, \nabla\cdot\phi_h^{n+1}) - \nu(\nabla\eta^{n+1}, \nabla\phi_h^{n+1}) - \gamma(\nabla\cdot\eta^{n+1}, \nabla\cdot\phi_h^{n+1}), \end{aligned} \tag{3.13}$$

phidiff0

where $r_h \in Q_h$ is arbitrary, and we used that $b(v_h^n, \phi_h^{n+1}, \phi_h^{n+1}) = 0$ and $(\eta^{n+1} - \eta^n, \phi_h^{n+1}) = 0$.

Many of these terms are bounded in a similar manner as in the case of backward Euler FEM for NSE, for example as in [35, 43, 20]. Using these techniques (which mainly consist of carefully constructed Hölder, Young, Cauchy-Schwarz, and Sobolev inequalities), we majorize all right side terms except the fifth and sixth terms to obtain

$$\begin{aligned}\frac{1}{2\Delta t}[\|\phi_h^{n+1}\|^2 - \|\phi_h^n\|^2 + \|\phi_h^{n+1}-\phi_h^n\|^2] &+ \frac{11\nu}{16}\|\nabla\phi_h^{n+1}\|^2 + \mu(I_H(\phi_h^{n+1}), \phi_h^{n+1}) + \frac{\gamma}{2}\|\nabla\cdot\phi_h^{n+1}\|^2\\ &\leq \nu^{-1}\Delta t^2\|u_{tt}(t^*)\|_{-1}^2 + 4M^2\nu^{-1}\Delta t^2\|\nabla u_t(t^*)\|^2\|\nabla u^n\|^2 + 4M^2\nu^{-1}\|\nabla v_h^n\|^2\|\nabla\eta^{n+1}\|^2\\ &\quad + 4M^2\nu^{-1}\|\nabla\eta^n\|^2\|\nabla u^{n+1}\|^2 - b(\phi_h^n, u^{n+1}, \phi_h^{n+1}) - \mu(I_H(\eta^{n+1}), \phi_h^{n+1})\\ &\quad + \gamma^{-1}\|p^{n+1} - r_h\|^2 + 4\nu\|\nabla\eta^{n+1}\|^2 + \gamma^{-1}\|\nabla\cdot\eta^{n+1}\|^2. \end{aligned}$$

Adding and subtracting $\phi_h^{n+1}$ to $I_H(\phi_h^{n+1})$, and using regularity assumptions on $u$, this reduces the bound to

$$\begin{aligned}\frac{1}{2\Delta t}[\|\phi_h^{n+1}\|^2 - \|\phi_h^n\|^2 + \|\phi_h^{n+1}-\phi_h^n\|^2] + \frac{11\nu}{16}\|\nabla\phi_h^{n+1}\|^2 + \mu\|\phi_h^{n+1}\|^2 + \frac{\gamma}{2}\|\nabla\cdot\phi_h^{n+1}\|^2 \\ \le C(1+M^2)\nu^{-1}\Delta t^2 + 4M^2\nu^{-1}\|\nabla v_h^n\|^2\|\nabla\eta^{n+1}\|^2 + 4CM^2\nu^{-1}\|\nabla\eta^n\|^2 \\ + \gamma^{-1}\|p^{n+1}-r_h\|^2 + 4\nu\|\nabla\eta^{n+1}\|^2 + \gamma\|\nabla\cdot\eta^{n+1}\|^2 \\ + |b(\phi_h^n, u^{n+1}, \phi_h^{n+1})| + \mu|(I_H(\eta^{n+1}),\phi_h^{n+1})| + \mu|(I_H(\phi_h^{n+1}) - \phi_h^{n+1}, \phi_h^{n+1})|. \end{aligned} \tag{3.14}$$

phidiff2

To bound the third to last term in (3.14), we begin by adding and subtracting $\phi_h^{n+1}$ to its first argument, and get

$$|b(\phi_h^n, u^{n+1}, \phi_h^{n+1})| \le |b(\phi_h^{n+1}-\phi_h^n, u^{n+1}, \phi_h^{n+1})| + |b(\phi_h^{n+1}, u^{n+1}, \phi_h^{n+1})|. \tag{3.15}$$

dp1

For both terms in (3.15), we use Lemma 2.1 and Young's inequality to obtain the bounds

$$\begin{aligned}|b(\phi_h^n - \phi_h^{n+1}, u^{n+1}, \phi_h^{n+1})| &\le M\|\phi_h^n - \phi_h^{n+1}\|\left(\|\nabla u^{n+1}\|_{L^3} + \|u^{n+1}\|_{L^\infty}\right)\|\nabla\phi_h^{n+1}\| \\ &\le 4M^2\nu^{-1}\|\phi_h^{n+1}-\phi_h^n\|^2(\|\nabla u^{n+1}\|_{L^3}^2 + \|u^{n+1}\|_{L^\infty}^2) + \frac{\nu}{16}\|\nabla\phi_h^{n+1}\|^2,\end{aligned}$$

and

$$\begin{aligned}b(\phi_h^{n+1}, u^{n+1}, \phi_h^{n+1}) &\le C\|\phi_h^{n+1}\|\left(\|\nabla u^{n+1}\|_{L^3} + \|u^{n+1}\|_{L^\infty}\right)\|\nabla\phi_h^{n+1}\| \\ &\le 4M^2\nu^{-1}\|\phi_h^{n+1}\|^2\left(\|\nabla u^{n+1}\|_{L^3}^2 + \|u^{n+1}\|_{L^\infty}^2\right) + \frac{\nu}{16}\|\nabla\phi_h^{n+1}\|^2.\end{aligned}$$

For the second to last term in (3.14), Cauchy-Schwarz and Young inequalities, along with (2.3), imply that

$$\begin{aligned}\mu(I_H(\eta^{n+1}),\phi_h^{n+1}) &\le \mu\|I_H(\eta^{n+1})\|\|\phi_h^{n+1}\|^2 \\ &\le C\mu\|\eta^{n+1}\|^2 + \frac{\mu}{4}\|\phi_h^{n+1}\|^2.\end{aligned}$$

For the last term in (3.14), we apply Cauchy-Schwarz and Young's inequalities and (2.2) to get

$$\begin{aligned}\mu\left|(I_H(\phi_h^{n+1}) - \phi_h^{n+1}, \phi_h^{n+1})\right| &\le \mu\|I_H(\phi_h^{n+1}) - \phi_h^{n+1}\|\|\phi_h^{n+1}\| \\ &\le \mu C_I h\|\nabla\phi_h^{n+1}\|\|\phi_h^{n+1}\| \\ &\le \mu C_I^2 h^2\|\nabla\phi_h^{n+1}\|^2 + \frac{\mu}{4}\|\phi_h^{n+1}\|^2.\end{aligned}$$

Combining the above bounds, and recalling the definition of $\alpha$, reduces (3.14) to

$$\begin{aligned}\frac{1}{2\Delta t}[\|\phi_h^{n+1}\|^2 - \|\phi_h^n\|^2 + \|\phi_h^{n+1}-\phi_h^n\|^2] + \frac{\gamma}{2}\|\nabla\cdot\phi_h^{n+1}\|^2 \\ +\frac{\alpha}{2}\|\nabla\phi_h^{n+1}\|^2 + \left(\frac{\mu}{2} - 4M^2\nu^{-1}\left(\|\nabla u^{n+1}\|_{L^3}^2 + \|u^{n+1}\|_{L^\infty}^2\right)\right)\|\phi_h^{n+1}\|^2 \\ \le C(1+M^2)\nu^{-1}\Delta t^2 + 4M^2\nu^{-1}\|\nabla v_h^n\|^2\|\nabla\eta^{n+1}\|^2 + 4CM^2\nu^{-1}\|\nabla\eta^n\|^2 \\ + \gamma^{-1}\|p^{n+1}-r_h\|^2 + 4\nu\|\nabla\eta^{n+1}\|^2 + \gamma\|\nabla\cdot\eta^{n+1}\|^2 \\ + C\mu\|\eta^{n+1}\|^2 + 4M^2\nu^{-1}\|\phi_h^{n+1}-\phi_h^n\|^2(\|\nabla u^{n+1}\|_{L^3}^2 + \|u^{n+1}\|_{L^\infty}^2).\end{aligned} \tag{3.16}$$

phidiff2b

It remains to estimate the term $4M^2\nu^{-1}\|\nabla v_h^n\|^2\|\nabla\eta^{n+1}\|^2$. By adding and subtracting $u^n$ to $v_h^n$ and using the triangle inequality, we have that

$$\|\nabla v_h^n\| \le \|\nabla u^n\| + \|\nabla\eta^n\| + \|\nabla(\phi_h^{n+1}-\phi_h^n)\| + \|\nabla\phi_h^{n+1}\|.$$

Using interpolation estimates, we obtain the bound

$$\begin{aligned}\|\nabla v_h^n\|^2\|\nabla\eta^{n+1}\|^2 &\le C\Big(\|\nabla u^n\|^2\|\nabla\eta^{n+1}\|^2 + \|\nabla\eta^n\|^2\|\nabla\eta^{n+1}\|^2\\ &\quad +\|\nabla(\phi_h^{n+1}-\phi_h^n)\|^2\|\nabla\eta^{n+1}\|^2 + \|\nabla\phi_h^{n+1}\|^2\|\nabla\eta^{n+1}\|^2\Big)\\ &\le C\Big(h^{2k}U^2 + h^{4k}U^4 + h^{2k-2}U^2\|\phi_h^{n+1}-\phi_h^n\|^2 + h^{2k-2}U^2\|\phi_h^{n+1}\|^2\Big),\end{aligned}$$

where in the last step we used the inverse inequality. Using this in (3.16) gives us that

$$\begin{aligned}&\frac{1}{2\Delta t}[\|\phi_h^{n+1}\|^2 - \|\phi_h^n\|^2] + \frac{\gamma}{2}\|\nabla\cdot\phi_h^{n+1}\|^2 + \frac{\alpha}{2}\|\nabla\phi_h^{n+1}\|^2\\ &\quad+\|\phi_h^{n+1}-\phi_h^n\|^2\left(\frac{1}{2\Delta t} - CM^2\nu^{-1}h^{2k-2}U^2 - 4M^2\nu^{-1}\|\nabla u^{n+1}\|_{L^3}^2 + \|u^{n+1}\|_{L^\infty}^2\right)\\ &\quad+\left(\frac{\mu}{2} - CM^2\nu^{-1}h^{2k-2}U^2 - 4M^2\nu^{-1}\left(\|\nabla u^{n+1}\|_{L^3}^2 + \|u^{n+1}\|_{L^\infty}^2\right)\right)\|\phi_h^{n+1}\|^2\\ &\qquad\le C(1+M^2)\nu^{-1}\Delta t^2 + CM^2\nu^{-1}h^{2k}U^2 + CM^2\nu^{-1}h^{4k}U^4 + CM^2\nu^{-1}\|\nabla\eta^n\|^2\\ &\qquad\quad+\gamma^{-1}\|p^{n+1}-r_h\|^2 + 4\nu\|\nabla\eta^{n+1}\|^2 + \gamma\|\nabla\cdot\eta^{n+1}\|^2 + C\frac{\nu}{C_I^2h^2}\|\eta^{n+1}\|^2. \end{aligned} \tag{3.17}$$

phidiff2c

Using the assumptions on $\mu$ and $\Delta t$, we reduce the left hand side of (3.17) by dropping non-negative terms and using the Poincaré inequality, and the right hand side using interpolation properties for $\eta^n$ to get that

$$\begin{aligned}&\frac{1}{2\Delta t}[\|\phi_h^{n+1}\|^2 - \|\phi_h^n\|^2] + \frac{\alpha}{2}C_P^{-2}\|\nabla\phi_h^{n+1}\|^2\\ &\qquad\le C(1+M^2)\nu^{-1}\Delta t^2 + CM^2\nu^{-1}h^{2k}U^2 + CM^2\nu^{-1}h^{4k}U^4 + CM^2\nu^{-1}h^{2k}U^2\\ &\qquad\quad + C\gamma^{-1}h^{2k}P^2 + C\nu h^{2k}U^2 + C\gamma^{-1}h^{2k}U^2 + C\frac{\nu}{C_I^2h^2}h^{2k+2}U^2\\ &\qquad\le C\Big((1+M^2)\nu^{-1}\Delta t^2 + h^{2k}U^2(M^2\nu^{-1} + M^2\nu^{-1}h^{2k}U^2 + \nu + \gamma + \nu C_I^{-2}) + \gamma^{-1}h^{2k}P^2\Big). \end{aligned} \tag{3.18}$$

phidiff2d

Define the parameter $\lambda = \alpha C_P^{-2}$, and reduce (3.18) to

$$(1+2\lambda\Delta t)\|\phi_h^{n+1}\|^2 \le \|\phi_h^n\|^2 + \Delta t R, \tag{3.19}$$

phidiff2e

where

$$R = C\Big((1+M^2)\nu^{-1}\Delta t^2 + h^{2k}U^2(M^2\nu^{-1} + M^2\nu^{-1}h^{2k}U^2 + \nu + \gamma + \nu C_I^{-2})\Big).$$

Now using Lemma 2.5, we obtain

$$\|\phi_h^{n+1}\|^2 \leq \left(\frac{1}{1+2\lambda\Delta t}\right)^{n+1} \|\phi_h^0\|^2 + \frac{R}{2\lambda}.$$

Applying the triangle inequality completes the proof.

□

# 4 Extension to a second order temporal discretization

A BDF2 IMEX scheme for NSE with data assimilation is studied in this section. We prove well-posedness, and global in time stability and convergence. Similar results as the previous section are found, but here with second order temporal error. The second order IMEX-FEM algorithm is defined as follows.

bdf2alg1 **Algorithm 4.1.** Given $v_h^0$, $v_h^1 \in V_h$, $f \in L^\infty(0,\infty;L^2(\Omega))$, and $u \in L^\infty(0,\infty;L^2(\Omega))$, find $(v_h^{n+1}, q_h^{n+1}) \in (X_h, Q_h)$ for $n = 1, 2, ...$, satisfying

$$\begin{aligned}
\frac{1}{2\Delta t}\left(3v_h^{n+1} - 4v_h^n + v_h^{n-1}, \chi_h\right) + b(2v_h^n - v_h^{n-1}, v_h^{n+1}, \chi_h) - (q_h^{n+1}, \nabla\cdot\chi_h) & \\
+\gamma(\nabla\cdot v_h^{n+1}, \nabla\cdot\chi_h) + \nu(\nabla v_h^{n+1}, \nabla\chi_h) + \mu(I_H(v_h^{n+1} - u^{n+1}), \chi_h) &= (f^{n+1}, \chi_h), \quad (4.1)\\
(\nabla\cdot v_h^{n+1}, r_h) &= 0, \quad (4.2)
\end{aligned}$$

for all $(\chi_h, r_h) \in X_h \times Q_h$, with $I_H$ a given interpolation operator satisfying (2.2)-(2.3).

Well-posedness of this algorithm, and long time stability, follow in a similar manner to the backward Euler case. However, the treatment of the time derivative terms is much more delicate, and we use G-stability theory to aid in this. We state and prove the result now.

bilityBDF2 **Lemma 4.3.** *Suppose $\mu$ satisfies*

$$1 \leq \mu < \frac{\nu}{2C_I^2 h^2}.$$

*Then for any time step size $\Delta t > 0$, Algorithm 4.1 is well-posed globally in time, and solutions are nonlinearly long-time stable: for any $n > 1$,*

$$\begin{aligned}
&\left(C_l^2\left(\|v_h^{n+1}\|^2 + \|v_h^n\|^2\right) + \frac{\alpha\Delta t}{2}\|\nabla v_h^{n+1}\|^2 + \frac{\mu\Delta t}{4}\|v_h^{n+1}\|^2\right)\\
&\quad\leq \left(C_u^2\|v_h^1\|^2 + \|v_h^0\|^2 + \frac{\alpha\Delta t}{2}\|\nabla v_h^1\|^2 + \frac{\mu\Delta t}{4}\|v_h^1\|^2\right)\left(\frac{1}{1+\lambda\Delta t}\right)^{n+1} + C\lambda^{-1}\nu^{-1}F^2 + C\lambda^{-1}\mu U^2.
\end{aligned}$$

*where* $\lambda = \min\{2\Delta t^{-1}, \frac{\mu C_l^2}{4}, \frac{\alpha C_P^{-2} C_l^2}{2}\}$ *and* $U := \|u\|^2_{L^\infty(0,\infty;L^2)}$.

**Remark 4.4.** We remark that $\mu$ does not scale with $h$, once $h$ is sufficiently small for a $\mu$ to exist within the restrictions. Thus as the discretization parameters $h$ and $\Delta t$ go to zero, $\mu$ can be considered a constant.

*Proof.* Choose $\chi_h = v_h^{n+1}$ in (4.1) and use (2.7) to obtain the bound

$$\frac{1}{2\Delta t}\left(\|[v_h^{n+1};v_h^n]\|_G^2\right) + \nu\|\nabla v_h^{n+1}\|^2 + \mu(I_H(v_h^{n+1}), v_h^{n+1}) \\ \leq \frac{1}{2\Delta t}\left(\|[v_h^n;v_h^{n-1}]\|_G^2\right) + \left|\left(f^{n+1}, v_h^{n+1}\right)\right| + \mu(I_H(u^{n+1}), v_h^{n+1}).$$

noting that we dropped the non-negative terms $\gamma\|\nabla\cdot v_h^{n+1}\|^2$ and $\frac{1}{4\Delta t}\|v_h^{n+1} - 2v_h^n + v_h^{n-1}\|^2$ from the left hand side, and that the nonlinear term and pressure term drop. Analyzing the nudging, viscous and forcing terms just as in the backward Euler case, and multiplying both sides by $2\Delta t$ we reduce the bound to

$$\left(\|[v_h^{n+1};v_h^n]\|_G^2\right) + 2\alpha\Delta t\|\nabla v_h^{n+1}\|^2 + \mu\Delta t\|v_h^{n+1}\|^2 \leq \left(\|[v_h^n;v_h^{n-1}]\|_G^2\right) + \Delta t(2\nu^{-1}F^2 + C\mu U^2).$$

Next, drop the viscous term on the left hand side, and add $\frac{\mu\Delta t}{4}\|v_h^n\|^2 + \frac{\alpha\Delta t}{2}\|\nabla v_h^n\|^2$ to both sides. This gives

$$\left(\|[v_h^{n+1};v_h^n]\|_G^2 + \frac{\mu\Delta t}{4}\|v_h^{n+1}\|^2 + \frac{\alpha\Delta t}{2}\|\nabla v_h^{n+1}\|^2\right) \\ + \frac{\mu\Delta t}{4}\left(\|v_h^{n+1}\|^2 + \|v_h^n\|^2\right) + \frac{\alpha\Delta t}{2}\left(\|\nabla v_h^{n+1}\|^2 + \|\nabla v_h^n\|^2\right) + \frac{\mu\Delta t}{2}\|v_h^{n+1}\|^2 + \alpha\Delta t\|\nabla v_h^{n+1}\|^2 \\ \leq \left(\|[v_h^n;v_h^{n-1}]\|_G^2 + \frac{\mu\Delta t}{4}\|v_h^n\|^2 + \frac{\alpha\Delta t}{2}\|\nabla v_h^n\|^2\right) + \Delta t(2\nu^{-1}F^2 + C\mu U^2),$$

which reduces using Poincaré's inequality and G-norm equivalence to

$$\left(\|[v_h^{n+1};v_h^n]\|_G^2 + \frac{\mu\Delta t}{4}\|v_h^{n+1}\|^2 + \frac{\alpha\Delta t}{2}\|\nabla v_h^{n+1}\|^2\right) \\ + \frac{\mu\Delta t C_l^2}{4}\|[v_h^{n+1};v_h^n]\|_G^2 + \frac{\alpha\Delta t C_P^{-2}C_l^2}{2}\|[v_h^{n+1};v_h^n]\|_G^2 + \frac{\mu\Delta t}{2}\|v_h^{n+1}\|^2 + \alpha\Delta t\|\nabla v_h^{n+1}\|^2 \\ \leq \left(\|[v_h^n;v_h^{n-1}]\|_G^2 + \frac{\mu\Delta t}{4}\|v_h^n\|^2 + \frac{\alpha\Delta t}{2}\|\nabla v_h^n\|^2\right) + \Delta t(2\nu^{-1}F^2 + C\mu U^2),$$

Thus there exists $\lambda = \min\{2\Delta t^{-1}, \frac{\mu C_l^2}{4}, \frac{\alpha C_P^{-2}C_l^2}{2}\}$ such that

$$(1+\lambda\Delta t)\left(\|[v_h^{n+1};v_h^n]\|_G^2 + \frac{\alpha\Delta t}{2}\|\nabla v_h^{n+1}\|^2 + \frac{\mu\Delta t}{4}\|v_h^{n+1}\|^2\right) \\ \leq \left(\|[v_h^n;v_h^{n-1}]\|_G^2 + \frac{\alpha\Delta t}{2}\|\nabla v_h^n\|^2 + \frac{\mu\Delta t}{4}\|v_h^n\|^2\right) + \Delta t(2\nu^{-1}F^2 + C\mu U^2),$$

and so by Lemma 2.5,

$$\left(\|[v_h^{n+1};v_h^n]\|_G^2 + \frac{\alpha\Delta t}{2}\|\nabla v_h^{n+1}\|^2 + \frac{\mu\Delta t}{4}\|v_h^{n+1}\|^2\right) \\ \leq \left(\|[v_h^1;v_h^0]\|_G^2 + \frac{\alpha\Delta t}{2}\|\nabla v_h^1\|^2 + \frac{\mu\Delta t}{4}\|v_h^1\|^2\right)\left(\frac{1}{1+\lambda\Delta t}\right)^{n+1} \\ + C\nu^{-1}F^2 + C\mu U^2.$$

Applying G-norm equivalence completes the proof of stability.

Since the scheme is linear and finite dimensional at each time step, this uniform in $n$ stability result gives existence and uniqueness of the algorithm at every time step. $\square$

Proving a long time accuracy result for Algorithm 4.1 follows in a similar manner to the first order result in the previous section. The key difference is the time derivative terms, which we handle with the G-stability theory in a manner similar as in the stability proof.

bdf2conv2 **Theorem 4.5.** *Let $u, p$ solve the NSE* (1.1)-(1.2) *with given $f \in L^\infty(0,\infty;L^2(\Omega))$ and $u_0 \in L^2(\Omega)$, with $u \in L^\infty(0,\infty;H^{k+1}(\Omega))$, $p \in L^\infty(0,\infty;H^k(\Omega))$ $(k \geq 1)$, $u_{tt} \in L^\infty(0,\infty;L^2(\Omega))$, and $u_{ttt} \in L^\infty(0,\infty;H^1(\Omega))$. Denote $U := |u|_{L^\infty(0,\infty;H^{k+1})}$ and $P := |p|_{L^\infty(0,\infty;H^k)}$. Assume the time step size satisfies*

$$\Delta t < CM^2\nu^{-1}\left(h^{2k-3}U^2 + \|\nabla u^{n+1}\|_{L^3}^2 + \|u^{n+1}\|_{L^\infty}^2\right)^{-1},$$

*and the parameter $\mu$ satisfies*

$$CM^2\nu^{-1}\left(h^{2k-3}U^2 + \|\nabla u^{n+1}\|_{L^3}^2 + \|u^{n+1}\|_{L^\infty}^2\right) < \mu < \frac{2\nu}{C_I^2 h^2}.$$

*Then there exists a $\lambda > 0$ (independent of $h$ and $\Delta t$) such that the error in solutions to Algorithm 4.1 satisfies, for any $n$,*

$$\|u^n - v_h^n\|^2 \leq \left(\frac{1}{1+\lambda\Delta t}\right)^n \|u_0 - v_h^0\|^2 + \frac{R}{\lambda},$$

*where* $R = C\nu^{-1}(1+M^2)\Delta t^4 + Ch^{2k}\left(\gamma^{-1}P^2 + (\nu + \gamma + M^2\nu^{-1} + M^2\nu^{-1}h^{2k}U^2 + \nu C_I^{-2})U^2\right)$.

**Remark 4.6.** For the case of Taylor-Hood or Scott-Vogelius elements and 0 initial condition in the DA algorithm, the result of the theorem reduces to

$$\|u^n - v_h^n\| \leq C\left(\left(\frac{1}{1+2\lambda\Delta t}\right)^{n/2}\|u_0\| + \Delta t^2 + h^k\right).$$

**Remark 4.7.** Similar to the first order case, the time step restriction is a consequence of the IMEX time stepping. If we instead consider the fully nonlinear scheme, then no $\Delta t$ restriction is required for a similar result to hold. However, there is seemingly a time step restriction necessary for solution uniqueness for the nonlinear scheme.

**Remark 4.8.** Just as in the first order case, grad-div stabilization reduces the effect of the pressure on the $L^2$ DA solution error. With grad-div, the contribution of the error term is $h^k\gamma^{-1/2}|p|_{L^\infty(0,\infty;H^k)}$, but without it, the $\gamma^{-1/2}$ would be replaced by a $\nu^{-1/2}$. If divergence-free elements were used, then this term would completely vanish. We show in numerical experiment 2 below case where a DA simulation will fail with Taylor-Hood elements with $\gamma = 0, 1, 10$, but will work very well with Scott-Vogelius elements.

*Proof.* Throughout this proof, the constant $C$ will denote a generic constant, possibly changing at each instance, that is independent of $h$, $\mu$, and $\Delta t$.

Using Taylor's theorem, the NSE (true) solution satisfies, for all $\chi_h \in X_h$,

$$\frac{1}{2\Delta t}\left(3u^{n+1} - 4u^n + u^{n-1}, \chi_h\right) + b(2u^n - u^{n-1}, u^{n+1}, \chi_h) - (p^{n+1}, \nabla\cdot\chi_h) + \gamma(\nabla\cdot u^{n+1}, \nabla\cdot\chi_h) + \nu(\nabla u^{n+1}, \nabla\chi_h) = (f^{n+1}, \chi_h) + C\Delta t^2(u_{ttt}(t^*), \chi_h) + C\Delta t^2 b(u_{tt}(t^{**}), u^{n+1}, \chi_h), \quad (4.9)$$ nsetrue3_n

where $t^*, t^{**} \in [t^{n-1}, t^{n+1}]$. Subtracting (4.1) from (3.11) yields the following difference equation, with $e^n := u^n - v_h^n$:

$$\begin{aligned}\frac{1}{2\Delta t}&(3e^{n+1} - 4e^n + e^{n-1}, \chi_h) + \nu(\nabla e^{n+1}, \nabla\chi_h) + \mu(I_H(e^{n+1}), \chi_h) + \gamma(\nabla\cdot e^{n+1}, \nabla\cdot\chi_h)\\ &= C\Delta t(u_{ttt}(t^*), \chi_h) + C\Delta t^2(u_{tt}(t^{**})\cdot\nabla u^{n+1}, \chi_h) - (P^{n+1}, \nabla\cdot\chi_h) + b(2v_h^n - v_h^{n-1}, e^{n+1}, \chi_h)\\ &\quad + b(2e^n - e^{n-1}, u^{n+1}, \chi_h).\end{aligned}$$

We decompose the error into a piece inside the discrete space $V_h$ and one outside of it by adding and subtracting $P_{V_h}^{L^2}(u^n)$. Denote $\eta^n := u^n - P_{V_h}^{L^2}(u^n)$ and $\phi_h^n := P_{V_h}^{L^2}(u^n) - v_h^n$. Then $e^n = \eta^n + \phi_h^n$ with $\phi_h^n \in V_h$, and we choose $\chi_h = \phi_h^{n+1}$. Using identity 2.7 with $\psi_\phi := (\phi_h^n, \phi_h^{n+1})^T$, the difference equation becomes

$$\begin{aligned}\frac{1}{2\Delta t}&[\|\psi_\phi^{n+1}\|_G^2 - \|\psi_\phi^n\|_G^2] + \frac{1}{4\Delta t}\|\phi_h^{n+1} - 2\phi_h^n + \phi_h^{n-1}\|^2 + \nu\|\nabla\phi_h^{n+1}\|^2 + \mu\|\phi_H^{n+1}\|^2 + \gamma\|\nabla\cdot\phi_h^{n+1}\|^2\\ &= C\Delta t^2(u_{ttt}(t^*), \phi_h^{n+1}) + C\Delta t^2(u_{tt}(t^{**})\cdot\nabla u^{n+1}, \phi_h^{n+1}) - (P^{n+1}, \nabla\cdot\phi_h^{n+1})\\ &\quad + b(2\phi_h^n - \phi_h^{n-1}, u^{n+1}, \phi_h^{n+1}) + b(2\eta^n - \eta^{n-1}, u^{n+1}, \phi_h^{n+1}) + b(2v_h^n - v_h^{n-1}, \eta^{n+1}, \phi_h^{n+1})\\ &\quad - \nu(\nabla\eta^{n+1}, \nabla\phi_h^{n+1}) - \mu(I_H\phi_h^{n+1} - \phi_h^{n+1}, \phi_h^{n+1}) - \mu(I_H\eta^{n+1}, \phi_h^{n+1})\\ &\quad - \gamma(\nabla\cdot\eta^{n+1}, \nabla\cdot\phi_h^{n+1}),\end{aligned} \tag{4.10}$$

bdf2diff

where we have added and subtracted $\phi_h^{n+1}$ in the interpolation term on the left hand side. We can now bound the right hand side of (4.10). For the first nonlinear term in (4.10), we add and subtract $\phi_h^{n+1}$ in the first argument to get

$$b(2\phi_h^n - \phi_h^{n-1}, u^{n+1}, \phi_h^{n+1}) = b(\phi_h^{n+1}, u^{n+1}, \phi_h^{n+1}) - b(\phi_h^{n+1} - 2\phi_h^n + \phi_h^{n-1}, u^{n+1}, \phi_h^{n+1}). \tag{4.11}$$

nl3

We bound the two resulting terms using Lemma 2.1 and Young's inequality, via

$$b(\phi_h^{n+1}, u^{n+1}, \phi_h^{n+1}) \le CM\nu^{-1}(\|\nabla u^{n+1}\|_{L^3}^2 + \|u^{n+1}\|_{L^\infty}^2)\|\phi_h^{n+1}\|^2 + \frac{\nu}{16}\|\nabla\phi_h^{n+1}\|^2,$$

and

$$\begin{aligned}b(\phi_h^{n+1} &- 2\phi_h^n + \phi_h^{n-1}, u^{n+1}, \phi_h^{n+1})\\ &\le CM\nu^{-1}(\|\nabla u^{n+1}\|_{L^3}^2 + \|u^{n+1}\|_{L^\infty}^2)\|\phi_h^{n+1} - 2\phi_h^n + \phi_h^{n-1}\|^2 + \frac{\nu}{16}\|\nabla\phi_h^{n+1}\|^2.\end{aligned}$$

The second nonlinear term in (4.10) is bounded with this same technique:

$$\begin{aligned}b(2\eta^n &- \eta^{n-1}, u^{n+1}, \phi_h^{n+1})\\ &\le CM^2\nu^{-1}(\|\nabla u^{n+1}\|_{L^3}^2 + \|u^{n+1}\|_{L^\infty}^2)\|2\eta^n - \eta^{n-1}\|^2 + \frac{\nu}{16}\|\nabla\phi_h^{n+1}\|^2.\end{aligned}$$

The last nonlinear term in (4.10) requires a bit more work, and we start by adding and subtracting $2u^n - u^{n-1}$ in the first component, which yields

$$\begin{aligned}b(2v_h^n - v_h^{n-1}, \eta^{n+1}, \phi_h^{n+1}) &= b(2u^n - u^{n-1}, \eta^{n+1}, \phi_h^{n+1}) + b(2e^n - e^{n-1}, \eta^{n+1}, \phi_h^{n+1})\\ &= b(2u^n - u^{n-1}, \eta^{n+1}, \phi_h^{n+1}) + b(2\phi_h^n - \phi_h^{n-1}, \eta^{n+1}, \phi_h^{n+1})\\ &\quad + b(2\eta^n - \eta^{n-1}, \eta^{n+1}, \phi_h^{n+1}).\end{aligned} \tag{4.12}$$

nl4

The first and third terms on the right hand side of (4.12) are bounded in the same way, using Lemma 2.1 and Young's inequality, to get that

$$b(2u^n - u^{n-1}, \eta^{n+1}, \phi_h^{n+1}) \leq C\nu^{-1}M^2\|\nabla(2u^n - u^{n-1})\|^2\|\nabla\eta^{n+1}\|^2 + \frac{\nu}{16}\|\nabla\phi_h^{n+1}\|^2,$$

$$b(2\eta^n - \eta^{n-1}, \eta^{n+1}, \phi_h^{n+1}) \leq C\nu^{-1}M^2\|\nabla(2\eta^n - \eta^{n-1})\|^2\|\nabla\eta^{n+1}\|^2 + \frac{\nu}{16}\|\nabla\phi_h^{n+1}\|^2,$$

For the second term in (4.12) we first add $\phi_h^{n+1}$ to the first argument to get

$$b(2\phi_h^n - \phi_h^{n-1}, \eta^{n+1}, \phi_h^{n+1}) = b(\phi_h^{n+1} - 2\phi_h^n + \phi_h^{n-1}, \eta^{n+1}, \phi_h^{n+1}) + b(\phi_h^{n+1}, \eta^{n+1}, \phi_h^{n+1}),$$

and then bound each resulting term using Lemma 2.1 and Young's inequality:

$$b(\phi_h^{n+1}, \eta^{n+1}, \phi_h^{n+1}) \leq CM^2\nu^{-1}(\|\eta^{n+1}\|_{L^\infty}^2 + \|\nabla\eta^{n+1}\|_{L^3}^2)\|\phi_h^{n+1}\|^2 + \frac{\nu}{16}\|\nabla\phi_h^{n+1}\|^2,$$

$$\begin{aligned} b(\phi_h^{n+1} - 2\phi_h^n + \phi_h^{n-1}, &\eta^{n+1}, \phi_h^{n+1}) \\ &\leq CM^2\nu^{-1}(\|\eta^{n+1}\|_{L^\infty}^2 + \|\nabla\eta^{n+1}\|_{L^3}^2)\|\phi_h^{n+1} - 2\phi_h^n + \phi_h^{n-1}\|^2 + \frac{\nu}{16}\|\nabla\phi_h^{n+1}\|^2. \end{aligned}$$

Collecting the above bounds, we can reduce (4.10) to

$$\begin{aligned} &\frac{1}{2\Delta t}[\|\psi_\phi^{n+1}\|_G^2 - \|\psi_\phi^n\|_G^2] + \frac{9\nu}{16}\|\nabla\phi_h^{n+1}\|^2 + \gamma\|\nabla\cdot\phi_h^{n+1}\|^2 \\ &+\left(\frac{1}{4\Delta t} - CM^2\nu^{-1}(\|\eta^{n+1}\|_{L^\infty}^2 + \|\nabla\eta^{n+1}\|_{L^3}^2 + \|u^{n+1}\|_{L^\infty}^2 + \|\nabla u^{n+1}\|^2)\right)\|\phi_h^{n+1} - 2\phi_h^n + \phi_h^{n-1}\|^2 \\ &+\left(\mu - CM^2\nu^{-1}(\|\eta^{n+1}\|_{L^\infty}^2 + \|\nabla\eta^{n+1}\|_{L^3}^2 + \|u^{n+1}\|_{L^\infty}^2 + \|\nabla u^{n+1}\|^2)\right)\|\phi_h^{n+1}\|^2 \\ &\leq C\Delta t^2|(u_{ttt}(t^*), \phi_h^{n+1})| + C\Delta t^2|(u_{tt}(t^{**})\cdot\nabla u^{n+1}, \phi_h^{n+1})| + |(p^{n+1} - r_h, \nabla\cdot\phi_h^{n+1})| \\ &+ \nu|(\nabla\eta^{n+1}, \nabla\phi_h^{n+1})| + \mu|(I_H\phi_h^{n+1} - \phi_h^{n+1}, \phi_h^{n+1})| + \mu|(I_H\eta^{n+1}, \phi_h^{n+1})| \\ &+ C\nu^{-1}M^2\|\nabla(2u^n - u^{n-1})\|^2\|\nabla\eta^{n+1}\|^2 + C\nu^{-1}M^2\|\nabla(2\eta^n - \eta^{n-1})\|^2\|\nabla\eta^{n+1}\|^2 \\ &+ CM^2\nu^{-1}(\|\nabla u^{n+1}\|_{L^3}^2 + \|u^{n+1}\|_{L^\infty}^2)\|2\eta^n - \eta^{n-1}\|^2 + \gamma|(\nabla\cdot\eta^{n+1}, \nabla\cdot\phi_h^{n+1})|. \end{aligned} \tag{4.13}$$

bdf2diff1

Now using interpolation estimates (and implicitly also the inverse inequality) along with regularity assumptions, we obtain

$$\begin{aligned} &\frac{1}{2\Delta t}[\|\psi_\phi^{n+1}\|_G^2 - \|\psi_\phi^n\|_G^2] + \frac{9\nu}{16}\|\nabla\phi_h^{n+1}\|^2 + \gamma\|\nabla\cdot\phi_h^{n+1}\|^2 \\ &+\left(\frac{1}{4\Delta t} - CM^2\nu^{-1}(h^{2k-3}U^2 + \|u^{n+1}\|_{L^\infty}^2 + \|\nabla u^{n+1}\|^2)\right)\|\phi_h^{n+1} - 2\phi_h^n + \phi_h^{n-1}\|^2 \\ &+\left(\mu - CM^2\nu^{-1}(h^{2k-3}U^2 + \|u^{n+1}\|_{L^\infty}^2 + \|\nabla u^{n+1}\|^2)\right)\|\phi_h^{n+1}\|^2 \\ &\leq C\Delta t^2|(u_{ttt}(t^*), \phi_h^{n+1})| + C\Delta t^2|(u_{tt}(t^{**})\cdot\nabla u^{n+1}, \phi_h^{n+1})| + |(P^{n+1}, \nabla\cdot\phi_h^{n+1})| \\ &+ \nu|(\nabla\eta^{n+1}, \nabla\phi_h^{n+1})| + \mu|(I_H\phi_h^{n+1} - \phi_h^{n+1}, \phi_h^{n+1})| + \mu|(I_H\eta^{n+1}, \phi_h^{n+1})| \\ &+ CM^2\nu^{-1}h^{2k}U^2(1 + h^{2k}U^2) + +\gamma|(\nabla\cdot\eta^{n+1}, \nabla\cdot\phi_h^{n+1})|. \end{aligned} \tag{4.14}$$

bdf2diff2

Next we use the assumptions on $\Delta t$ and $\mu$, and apply bounds to the remaining right hand side terms just as in the backward Euler proof to get

$$\begin{aligned}
&\frac{1}{2\Delta t}[\|\psi_\phi^{n+1}\|_G^2 - \|\psi_\phi^n\|_G^2] + 2\alpha\|\nabla\phi_h^{n+1}\|^2 + \frac{\gamma}{2}\|\nabla\cdot\phi_h^{n+1}\|^2 \\
&\qquad \leq C\nu^{-1}(1+M^2)\Delta t^4 + Ch^{2k}\left(\gamma^{-1}P^2 + (\nu+\gamma+M^2\nu^{-1} + M^2\nu^{-1}h^{2k}U^2 + \nu C_I^{-2})U^2\right) \\
&\qquad = R. \qquad (4.15)
\end{aligned}$$

bdf2diff3

This implies, with Poincaré's inequality that

$$\|\psi_\phi^{n+1}\|_G^2 + 4C_l^2\Delta t\alpha C_P^{-2}\|\phi_h^{n+1}\|^2 \leq \|\psi_\phi^n\|_G^2 + \Delta t R.$$

From here, can can proceed just as in to the BDF2 long time stability proof above to obtain

$$\|\psi_\phi^{n+1}\|_G^2 \leq \|\psi_\phi^0\|_G^2\left(\frac{1}{1+\lambda\Delta t}\right) + \frac{R}{\lambda},$$

and now the triangle inequality and G-norm equivalence complete the proof. □

# 5 Numerical Experiments

We now present results of three numerical tests that illustrate the theory above, and also show the importance of a careful choice of discretization. That is, while the DA theory at the PDE level is critical, in a discretization there are additional consideration and restrictions that can make the difference of a simulation succeeding or failing. All of our tests use Algorithm 4.1, i.e. the BDF2 IMEX-FEM algorithm studied in section 4.

## 5.1 Numerical Experiment 1: Convergence to an analytical solution

For our first experiment, we illustrate the convergence theory above for Algorithm 4.1 to the chosen analytical solution on $\Omega = (0,1)^2$,

$$\begin{aligned}
u(x,y,t) &= (\cos(y+t), \sin(x-t))^T, \\
p(x,y,t) &= \sin(2\pi(x+t)).
\end{aligned}$$

We take $\nu = 0.01$, the forcing function $f$ is calculated from the continuous NSE, $\nu$, and the solution, and the initial velocity is taken to be $u_0 = u(x,y,0)$.

We compute on a uniform mesh with Taylor-Hood elements and Dirichlet boundary conditions, and for simplicity we take $\gamma = 0$, since the grad-div stabilization has little effect in this test problem. The interpolation operator $I_H$ is chosen to be the nodal interpolant onto constant functions on the same mesh used for velocity and pressure, and the initial conditions for the DA algorithm are set to zero.

Results are shown in figure 1, for $\mu = 1,\ 10,\ 100$ using $h = \frac{1}{32}$ and $\Delta t = 0.01$, by plotting the $L^2$ difference between the DA computed solution and the true solution versus time. We observe convergence up to about $10^{-4}$, which is the level of the discretization error for the chosen discretization. We observe that for larger choices of $\mu$, convergence to the true solution (up to discretization error) is much faster. However, we note that the long time accuracy is not affected by $\mu$.

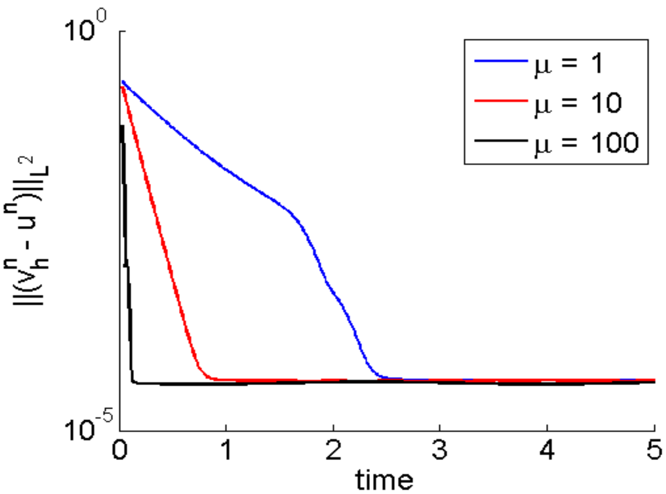


MU Figure 1: Shown above is a plot of convergence of the DA computed solutions to the true solution with increasing time $t$, for varying choices of the nudging parameter $\mu$.

Table 1 displays the convergence rates of the solutions to Algorithm 4.1 to the true solution; error is calculated using the $L^2$ norm. For these calculations, we take $\mu = 10$ and $\gamma = 1.0$ and run to an end time of $T = 4.0$. When observing the spatial convergence rates, we fix $\Delta t = 0.001$ and vary $h$, while for the temporal error we fix $h = \frac{1}{64}$ and vary $\Delta t$. We also test spatial and temporal convergence together, by reducing $h$ and $\Delta t$, but keeping the ratio $4h = \Delta t$. In all cases we observe second order convergence for spatial and temporal error, which is consistent with our analysis.

| $h$ | Error | Rate |
|---|---|---|
| 1/4 | 4.12E-3 | - |
| 1/8 | 5.16E-4 | 3.00 |
| 1/16 | 5.91E-5 | 3.13 |
| 1/32 | 8.71E-6 | 2.76 |
| 1/64 | 1.92E-6 | 2.18 |
| 1/128 | 4.75E-7 | 2.02 |

| $\Delta t$ | Error | Rate |
|---|---|---|
| 1 | 2.60E-3 | - |
| 1/2 | 3.63E-4 | 2.84 |
| 1/4 | 6.84E-5 | 2.41 |
| 1/8 | 1.52E-5 | 2.17 |
| 1/16 | 3.76E-6 | 2.02 |
| 1/32 | 1.09E-6 | 1.78 |

| $h$ | $\Delta t$ | Error | Rate |
|---|---|---|---|
| 1/4 | 1 | 4.69E-3 | - |
| 1/8 | 1/2 | 5.79E-4 | 3.02 |
| 1/16 | 1/4 | 9.16E-5 | 2.66 |
| 1/32 | 1/8 | 1.83E-5 | 2.32 |
| 1/64 | 1/16 | 4.38E-6 | 2.06 |
| 1/128 | 1/32 | 1.09E-6 | 2.00 |

hconv Table 1: Convergence rates of Algorithm 4.1 to the true solution with decreasing $h$ and fixed $\Delta t$ (left), fix $h$ and decreasing $\Delta t$ (middle), and also decreasing $h$ and $\Delta t$ at the same rate with $\Delta t = 4h$ (right).

## 5.2 Numerical Experiment 2: The no-flow test and pressure-robustness

For our second test, we show how pressure robustness of the discretization can have a dramatic impact on the DA solution. The test problem we consider is the so-called 'no-flow test', where the forcing function of the NSE is given by $Ra(0, y)^T$, where $Ra$ is a constant (the Rayleigh number), and with $Pr$ denoting the Prandtl number:

$$\frac{1}{Pr}(u_t + u \cdot \nabla u) + \nabla p - \Delta u = Ra(0, y)^T, \tag{5.1}$$ NF1

$$\nabla \cdot u = 0, \tag{5.2}$$ NF2

$$u|_{\partial\Omega} = 0. \tag{5.3}$$ NF3

This test problem corresponds to the physical situations of temperature driven flow (i.e. the Boussinesq system), with the temperature $\theta$ profile specified to be stratified, i.e. $f = Ra\theta e_2$ with $\theta = y$. Linear stratification is a natural steady state temperature profile. Since the forcing is potential, the solution to the system (5.1)-(5.3) with $u_0 = 0$ initial condition is given by

$$u = 0, \ p = \frac{Ra}{2}y^2,$$

for any $Pr > 0$, hence the name no-flow.

We consider Algorithm 4.1, applied to the no-flow test with $Pr = 1$ and $Ra = 10^5$ (although this may seem like a large choice of a constant, for Boussinesq problems of practical interest, this choice of $Ra$ is actually quite small). We use both Scott-Vogelius (SV) elements and Taylor-Hood (TH) elements, on a barycenter refined uniform discretization of the unit square with $h = \frac{1}{32}$. With TH elements, we use $\gamma = 0, 1, 10$. We take $I_H$ to be the nodal interpolant in $X_h$, and nudging parameter $\mu = 0.1$. The time step size is chosen to be $\Delta t = 0.025$, and solutions are computed up to end time $T = 0.8$, using the $X_h$ interpolant of $(x \cos y, -\sin y)^T$ for $v_h^0$, and $v_h^1$ is calculated from taking one step of the backward Euler DA scheme.

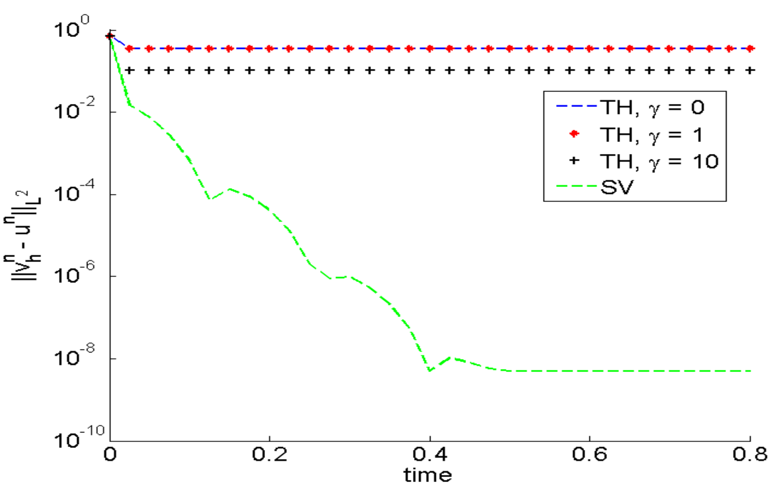


Ra5mu1 Figure 2: Shown above is error in DA solutions for the no-flow solution, with SV element and TH elements (with varying $\gamma$). TH elements give very bad results, while SV elements perform very well.

Results of the simulations are shown in figure 2, as $L^2$ error versus time, and we observe a dramatic difference between solutions from the two element choices. For TH elements, the results are poor due to the large pressure, which adversely affects the velocity error, *even using a very accurate interpolant*. With $\gamma = 10$, the TH solution is a little better, however, it is still on the order of $10^{-1}$ accuracy, which is not good. The SV solution, on the other hand, is excellent. Its error decays rapidly in time until it reaches a level around $10^{-8}$ and stays there. Thus we observe here that in DA algorithms, element choice can be critical for finding good results in Boussinesq type simulations

### 5.3 Numerical Experiment 3: 2D channel flow past a cylinder

For our last experiment, we consider Algorithm 4.1 applied to the common benchmark problem of 2D channel flow past a cylinder [42]. The domain is a $2.2 \times 0.41$ rectangular channel with a cylinder of radius 0.05 centered at $(0.2, 0.2)$, see figure 3. There is no external forcing, the kinematic viscosity is taken to be $\nu = 0.001$, no-slip boundary conditions are prescribed for the walls and the cylinder, while the inflow and outflow profiles are given by

$$
\begin{aligned}
u_1(0, y, t) &= u_1(2.2, y, t) = \frac{6}{0.41^2} y(0.41 - y), \\
u_2(0, y, t) &= u_2(2.2, y, t) = 0.
\end{aligned}
$$

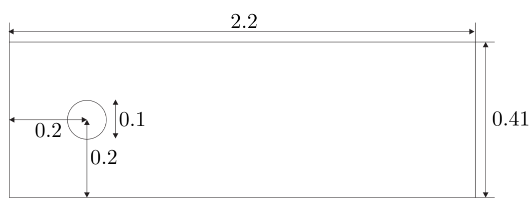


Figure 3: Shown above is the domain for the flow past a cylinder test problem.

Since we do not have access to a true solution for this problem, we instead use a computed solution. It is computed using the same BDF2-IMEX-FEM scheme as in Algorithm 4.1 but without nudging (i.e. $\mu = 0$), using Taylor-Hood elements on a mesh that provided 56,751 total degrees of freedom, a time step of $\Delta t = 0.025$, and with the simulation starting from rest ($u_h^0 = u_h^{-1} = 0$). A grad-div stabilization parameter of $\gamma = 1$ was used. We will refer to this solution as the DNS solution. Lift and drag calculations were performed for the computed solution and compared to the literature [42, 38], which verified the accuracy of the DNS.

For the lift and drag calculations, we used the formulas

$$
\begin{aligned}
c_d(t) &= 20 \int_S \left( \nu \frac{\partial u_{t_S}(t)}{\partial n} n_y - p(t) n_x \right) dS, \\
c_l(t) &= 20 \int_S \left( \nu \frac{\partial u_{t_S}(t)}{\partial n} n_x - p(t) n_y \right) dS,
\end{aligned}
$$

where $p(t)$ is the pressure, $u_{t_S}$ the tangential velocity $S$ the cylinder, and $n = \langle n_x, n_y \rangle$ the outward unit normal to the domain. For calculations, we use the global integral formula from [25].

For the DA algorithm, we start from $v_h^1 = v_h^0 = 0$, choose $\mu = 1$, the same spatial and temporal discretization parameters as the DNS, and begin assimilating with DNS data at $t = 4.0$. We compute two cases for DA, with the interpolation being done on the same mesh as for the simulations, one with a $P_2$ interpolant (i.e. $I_H$ acts as the identity operator on $X_h$) and also a $P_0$ interpolant.

First, we show contour plots of the DNS solution and DA solution at times $t = 4, 4.5, 6$ and 8 in figure 4. The two solutions look almost identical at $t = 4.0$. Figure 5 shows the $L^2$ difference between the DA and DNS solution, which goes to 0 as $t \to 4$.

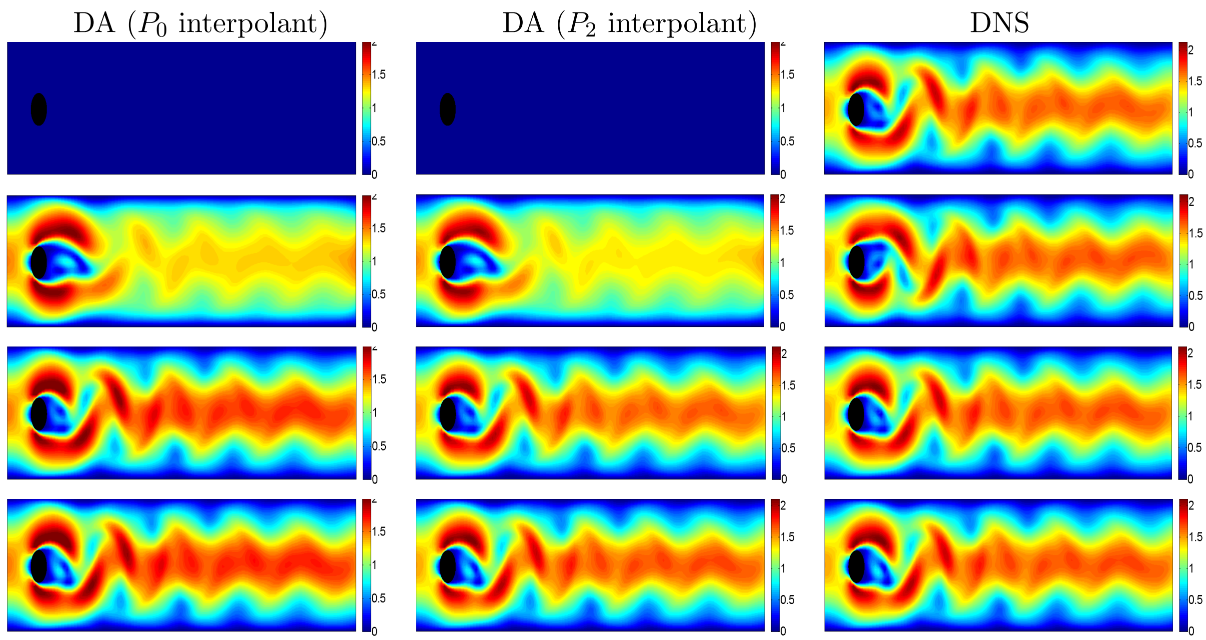


contourcyl Figure 4: Contour plots of DA and DNS velocity magnitudes at time 4 (4 is the initial time for DA), 0.5, 2, and 4.

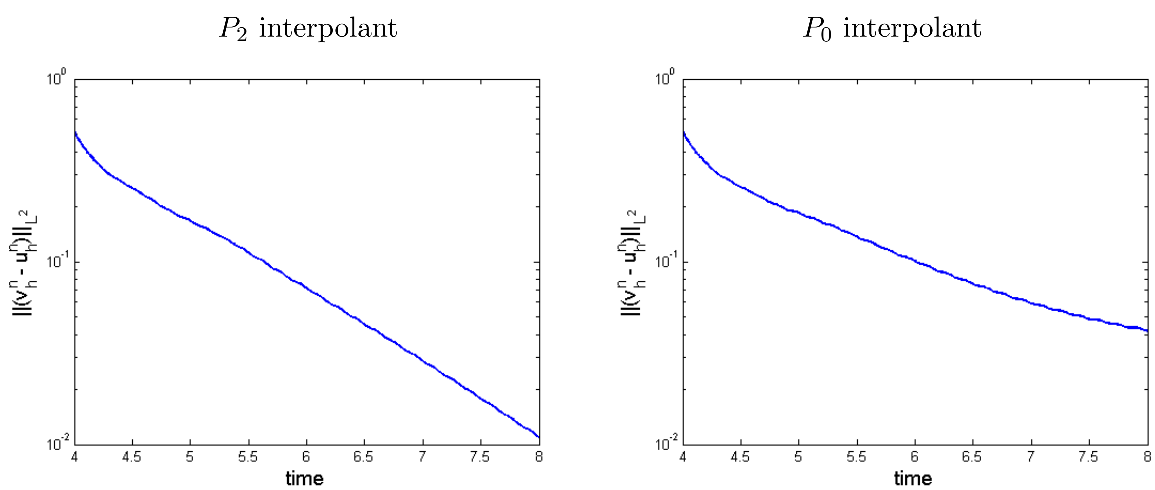


difference Figure 5: Shown above is $L^2$ difference between the DA and DNS solutions versus time, for the case of the $P_2$ interpolant (left) and $P_0$ interpolant (right).

Figure 6 shows plots of time versus the lift and drag coefficients, from time $t = 4.0$ to time $t = 8.0$. We can see that the lift and drag coefficients of the DA algorithm converge to those of the DNS algorithm at $t$ goes to 8.0. The results computed here agree well with the DNS results in [25], [23].

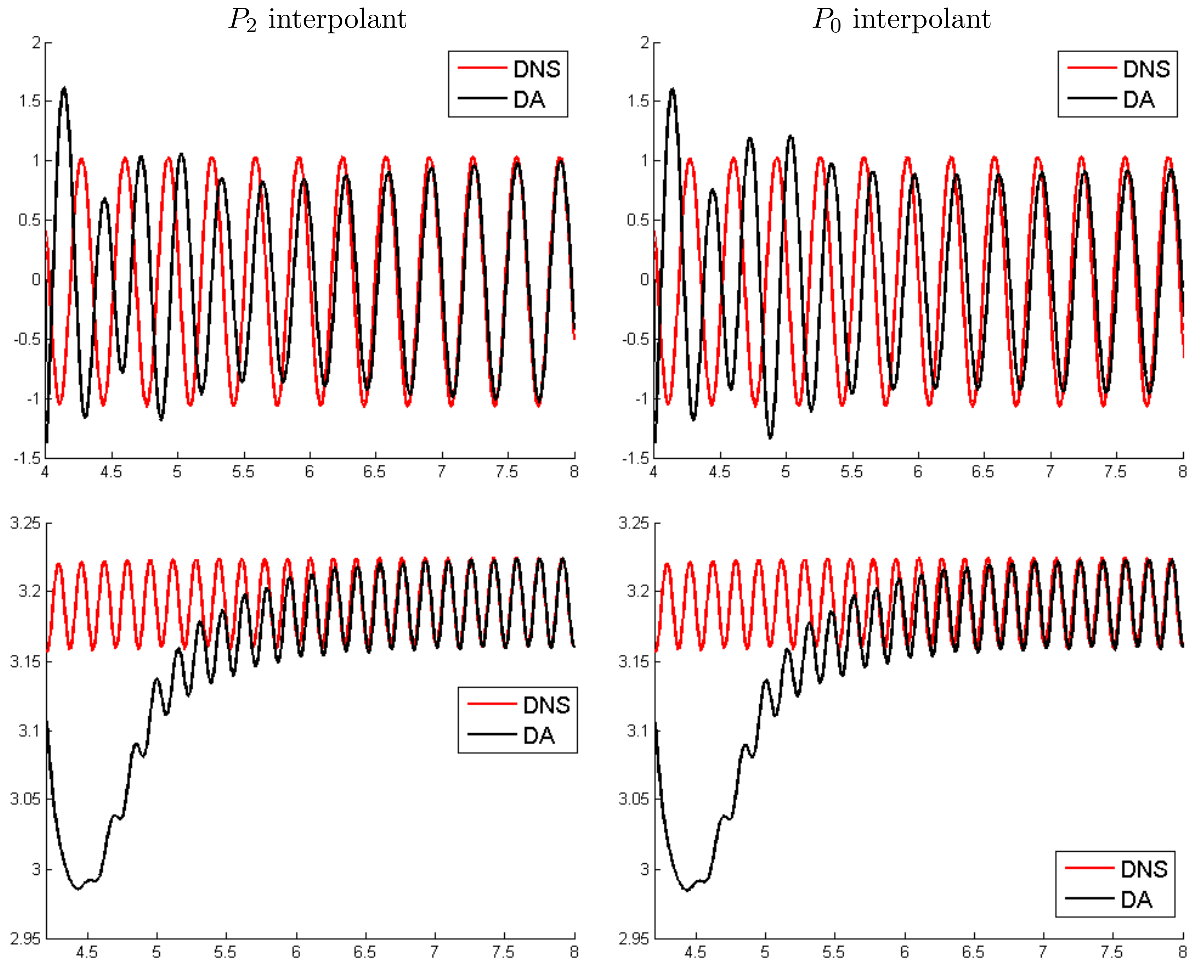


liftdrag Figure 6: Plots of lift (top) and drag (bottom) for DA and DNS solutions, using the $P_2$ (left) and $P_0$ interpolants.

## References

_Titi_2016 [1] Débora AF Albanez, Helena J Nussenzveig Lopes, and Edriss S Titi. Continuous data assimilation for the three-dimensional Navier–Stokes-$\alpha$ model. *Asymptotic Anal.*, 97(1-2):139–164, 2016.

oteit_2015 [2] M. U. Altaf, E. S. Titi, O. M. Knio, L. Zhao, M. F. McCabe, and I. Hoteit. Downscaling the 2D Benard convection equations using continuous data assimilation. *ArXiv e-prints*, December 2015.

_Titi_2014 [3] Abderrahim Azouani, Eric Olson, and Edriss S. Titi. Continuous data assimilation using general interpolant observables. *J. Nonlinear Sci.*, 24(2):277–304, 2014.

_Titi_2014 [4] Abderrahim Azouani and Edriss S. Titi. Feedback control of nonlinear dissipative systems by finite determining parameters—a reaction-diffusion paradigm. *Evol. Equ. Control Theory*, 3(4):579–594, 2014.

_Titi_2015 [5] Hakima Bessaih, Eric Olson, and Edriss S. Titi. Continuous data assimilation with stochastically noisy data. *Nonlinearity*, 28(3):729–753, 2015.

tinez_2017 [6] Animikh Biswas and Vincent R. Martinez. Higher-order synchronization for a data assimilation algorithm for the 2D Navier–Stokes equations. *Nonlinear Anal. Real World Appl.*, 35:132–157, 2017.

BKLSZ [7] D. Blömker, K.J.L. Law, A.M. Stuart, and K.C. Zygalakis. Accuracy and stability of the continuous-times 3dvar filter for the navier-stokes equations. *arXiv:1210.1594v2*.

_Titi_2001 [8] Chongsheng Cao, Ioannis G. Kevrekidis, and Edriss S. Titi. Numerical criterion for the stabilization of steady states of the Navier–Stokes equations. *Indiana Univ. Math. J.*, 50(Special Issue):37–96, 2001. Dedicated to Professors Ciprian Foias and Roger Temam (Bloomington, IN, 2000).

CHJ69 [9] J. Charney, M. Halem, and R. Jastrow. Use of incomplete historical data to infer the present state of the atmosphere. *Journal of Atmospheric Science*, 26:1160–1163, 1969.

CGSW13 [10] W. Chen, M. Gunzburger, D. Sun, and X. Wang. Efficient and long-time accurate second-order methods for stokes-darcy system. *SIAM Journal of Numerical Analysis*, 51:2563–2584, 2013.

heric_book [11] R. Daley. *Atmospheric Data Analysis*. Cambridge Atmospheric and Space Science Series. Cambridge University Press, 1993.

_Titi_2015 [12] Aseel Farhat, Michael S. Jolly, and Edriss S. Titi. Continuous data assimilation for the 2D Bénard convection through velocity measurements alone. *Phys. D*, 303:59–66, 2015.

16abridged [13] Aseel Farhat, Evelyn Lunasin, and Edriss S Titi. Abridged continuous data assimilation for the 2D Navier–Stokes equations utilizing measurements of only one component of the velocity field. *J. Math. Fluid Mech.*, 18(1):1–23, 2016.

2016benard [14] Aseel Farhat, Evelyn Lunasin, and Edriss S Titi. Data assimilation algorithm for 3D Bénard convection in porous media employing only temperature measurements. *Journal of Mathematical Analysis and Applications*, 438(1):492–506, 2016.

16_Charney [15] Aseel Farhat, Evelyn Lunasin, and Edriss S Titi. On the Charney conjecture of data assimilation employing temperature measurements alone: The paradigm of 3d planetary geostrophic model. *arXiv:1608.04770*, 2016.

Horizontal [16] Aseel Farhat, Evelyn Lunasin, and Edriss S. Titi. Continuous data assimilation for a 2D Bénard convection system through horizontal velocity measurements alone. *Journal of Nonlinear Science*, pages 1–23, 2017.

_Titi_2016 [17] Ciprian Foias, Cecilia F. Mondaini, and Edriss S. Titi. A discrete data assimilation scheme for the solutions of the two-dimensional Navier-Stokes equations and their statistics. *SIAM J. Appl. Dyn. Syst.*, 15(4):2109–2142, 2016.

_Titi_2014 [18] K. Foyash, M. S. Dzholli, R. Kravchenko, and È. S. Titi. A unified approach to the construction of defining forms for a two-dimensional system of Navier-Stokes equations: the case of general interpolating operators. *Uspekhi Mat. Nauk*, 69(2(416)):177–200, 2014.

_Titi_2015 [19] Masakazu Gesho, Eric Olson, and Edriss S. Titi. A computational study of a data assimilation algorithm for the two-dimensional Navier-Stokes equations. *Commun. Comput. Phys.*, 19(4):1094–1110, 2016.

GR86 [20] V. Girault and P.-A. Raviart. *Finite element methods for Navier-Stokes equations: Theory and Algorithms*. Springer-Verlag, 1986.

Vicol_2014 [21] Nathan Glatt-Holtz, Igor Kukavica, Vlad Vicol, and Mohammed Ziane. Existence and regularity of invariant measures for the three dimensional stochastic primitive equations. *J. Math. Phys.*, 55(5):051504, 34, 2014.

HW02 [22] E. Hairer and G. Wanner. *Solving Ordinary Differential II: Stiff and Differential-Algebraic Problems*. Springer, 2 edition, 2002.

HN12 [23] D. Hannasch and M. Neda. On the accruacy of the viscous form in simulations of incompressible flow problems. *Numer. Methods Partial Differ. Equ.*, 28:523–541, 2012.

_Titi_2011 [24] Kevin Hayden, Eric Olson, and Edriss S. Titi. Discrete data assimilation in the Lorenz and 2D Navier-Stokes equations. *Phys. D*, 240(18):1416–1425, 2011.

J04 [25] V. John. Reference values for drag and lift of a two dimensional time-dependent flow around a cylinder. *Int. J. Numer. Methods Fluids*, 44:777–788, 2002.

JLMNR17 [26] V. John, A. Linke, C. Merdon, M. Neilan, and L. G. Rebholz. On the divergence constraint in mixed finite element methods for incompressible flows. *SIAM Review*, 59(3):492–544, 2017.

_Titi_2017 [27] Michael S. Jolly, Vincent R. Martinez, and Edriss S. Titi. A data assimilation algorithm for the subcritical surface quasi-geostrophic equation. *Adv. Nonlinear Stud.*, 17(1):167–192, 2017.

_Titi_2015 [28] Michael S. Jolly, Tural Sadigov, and Edriss S. Titi. A determining form for the damped driven nonlinear Schrödinger equation—Fourier modes case. *J. Differential Equations*, 258(8):2711–2744, 2015.

02AtmModel [29] E. Kalnay. *Atmospheric Modeling, data assimilation and predictability*. Cambridge University Press, 2002.

03_DA_book [30] E. Kalnay. *Atmospheric Modeling, Data Assimilation and Predictability*. Cambridge University Press, 2003.

_KSE_DA_NL [31] A. Larios and Y. Pei. Nonlinear continuous data assimilation. (submitted) arXiv:1703.03546.

018_3D_NSE [32] A. Larios, Y. Pei, and E. S. Titi. A computational study of continuous data assimilation for the 3d navier-stokes equations. (preprint).

_Titi_2015 [33] Adam Larios, Evelyn Lunasin, and Edriss S. Titi. Global well-posedness for the Boussinesq-Voigt equations. (preprint) arXiv:1010.5024.

_2015_book [34] Kody Law, Andrew Stuart, and Konstantinos Zygalakis. *A Mathematical Introduction to Data Assimilation*, volume 62 of *Texts in Applied Mathematics*. Springer, Cham, 2015.

laytonbook [35] W. Layton. *Introduction to Finite Element Methods for Incompressible, Viscous Flow*. SIAM, Philadelphia, 2008.

_Titi_2015 [36] E. Lunasin and E. S. Titi. Finite determining parameters feedback control for distributed non-linear dissipative systems - a computational study. arXiv:1506.03709 [math.AP], (submitted).

belsi_2016 [37] Peter A Markowich, Edriss S Titi, and Saber Trabelsi. Continuous data assimilation for the three-dimensional Brinkman–Forchheimer-extended Darcy model. *Nonlinearity*, 29(4):1292, 2016.

MRXI17 [38] M. Mohebujjaman, L. Rebholz, X. Xie, and T. Iliescu. Energy balance and mass conservation in reduced order models of fluid flows. *Journal of Computational Physics*, 346:262–277, 2017.

_Titi_2017 [39] C. F. Mondaini and E. S. Titi. Postprocessing Galerkin method applied to a data assimilation algorithm: a uniform in time error estimate. 2016. (arXiv 1612.06998).

18_SIAM_NA [40] Cecilia F. Mondaini and Edriss S. Titi. Uniform-in-time error estimates for the postprocessing Galerkin method applied to a data assimilation algorithm. *SIAM J. Numer. Anal.*, 56(1):78–110, 2018.

_Titi_2003 [41] Eric Olson and Edriss S. Titi. Determining modes for continuous data assimilation in 2D turbulence. *J. Statist. Phys.*, 113(5-6):799–840, 2003. Progress in statistical hydrodynamics (Santa Fe, NM, 2002).

ST96 [42] M. Schäfer and S. Turek. The benchmark problem 'flow around a cylinder' flow simulation with high performance computer ii. *Notes on Numerical Fluid Mechanics*, 52:547–566, 1996.

T77 [43] R. Temam. *Navier-Stokes Equations: Theory and Numerical Analysis*. North Holland Publishing Company, New York, 1977.